

UC San Diego

UC San Diego Electronic Theses and Dissertations

Title

Investigating differential binding of ADP-ribose by macrodomains

Permalink

<https://escholarship.org/uc/item/4dq1f59d>

Author

Hollingsworth, Derek Raymond

Publication Date

2019

Peer reviewed|Thesis/dissertation

UNIVERSITY OF CALIFORNIA SAN DIEGO

Investigating differential binding of ADP-ribose by macrodomains

A Thesis submitted in partial satisfaction of the requirements for the degree Master of Science

in

Biology

by

Derek Raymond Hollingsworth

Committee in charge:

Professor Matthew Daugherty, Chair
Professor Eric Bennett
Professor Elina Zuniga

2019

©
Derek Raymond Hollingsworth, 2019
All rights reserved.

The Thesis of Derek Raymond Hollingsworth is approved, and it is acceptable in quality and form for publication on microfilm and electronically:

Chair

University of California San Diego

2019

TABLE OF CONTENTS

Signature Page	iii
Table of Contents	iv
List of Figures.....	v
List of Tables	vi
Abstract of Thesis.....	vii
Introduction	1
Materials and Methods	9
Results	12
Discussion.....	17
Figures and Tables.....	24
References	39

LIST OF FIGURES

Figure 1: Expression vector pAR041, expressing Af1521 macrodomain with N-terminal 6xHis tag in <i>E. coli</i>	26
Figure 2: Binding of 6xHis-Af1521 construct to Ni-NTA column.....	27
Figure 3: Purification of PARP10-FLAG by Ni-NTA column with bound macrodomain.....	28
Figure 4: Binding of various human and bacterial proteins to Ni-NTA column.....	29
Figure 5: Inability of PARP10 to bind to Ni-NTA column.....	30
Figure 6: Confirmation of inability of PARP10 to bind to Ni-NTA column.....	31
Figure 7: Expression vector pDL2259, expressing mCherry-macrodomain fusion proteins in mammalian cells.....	32
Figure 8: Localization of different mCherry-macrodomain fusion proteins.....	33
Figure 9: Localization of different combinations of PARP14 macrodomains.....	35
Figure 10: Localization of mCherry-macrodomain fusion proteins following arsenite exposure.....	37

LIST OF TABLES

Table 1: List of plasmids used in transient transfection experiments.....24

Table 2: List of stably-expressing, doxycycline-inducible cell lines generated.....25

ABSTRACT OF THE THESIS

Investigating differential binding of ADP-ribose by macrodomains

by

Derek Raymond Hollingsworth

Master of Science in Biology

University of California San Diego, 2019

Professor Matthew Daugherty, Chair

The post-translational modification ADP-ribosylation, whereby ADP-ribose subunits are attached to proteins to alter their function, has been previously implicated in processes including DNA damage repair and certain stress responses. However, the mediators of this modification are poorly understood; in particular, little is known about a diverse class of ADP-ribose binding domains called macrodomains, beyond a general affinity to bind to ADP-ribose. Experiments were thus undertaken to determine if different macrodomains show

differences in their ADP-ribose binding activity. In addition, as several members of the macrodomain family are suspected to be involved in some host-pathogen conflict, potential alterations of macrodomains' ADP-ribose binding in response to immunological signals were also investigated. Initial experiments utilized an Ni-NTA column to purify proteins based on their ability to bind to a macrodomain; although initial experiments proved that such a system could purify ADP-ribosylated proteins, further refinement to this system is needed. Further experiments to address this question of differential binding of ADP-ribose by macrodomains utilized fluorescent proteins fused to macrodomains, which allow for the localization of the macrodomain inside a cell to be observed. These experiments were successful in demonstrating that different macrodomains localize to different cellular compartments, suggesting that they each bind to different sets of ADP-ribosylated proteins. Experiments to identify alterations in ADP-ribosylation in cells following exposure to immunological signals, however, were unsuccessful. Refinement of a pulldown assay to purify ADP-ribosylated proteins would be advantageous for future exploration of macrodomain binding activity.

INTRODUCTION:

Research into regulation of cellular gene expression has identified systems by which the functioning of already-synthesized proteins can be altered. These systems, known as post-translational modifications (PTMs), can regulate protein functioning by altering “activity state, localization, turnover, and interactions with other proteins” (Gruhler & Jensen, 2003). In addition, PTMs can be regulated by different PTMs, thus creating complex webs of post-translational regulation of gene expression. (Legube & Trouche, 2003). PTMs are incredibly widespread: the PTM known as ADP-ribosylation, whereby ADP-ribose subunits are attached to a protein, has been identified in all three domains of life (Perina et al., 2014). This PTM, ADP-ribosylation, has been implicated in such critical cellular processes as DNA damage repair (mediated by PARP1 and PARP2), chromosomal segregation during mitosis (mediated by PARP5a), and certain stress responses (mediated by PARP16) (Aguilera-Gomez et al., 2016; Daugherty et al., 2014; Krishnakumar & Kraus, 2010).

Any PTM involving addition of small molecules to proteins requires three broad classes of functions: “writers,” to attach the modification to the target protein, “readers,” to identify the modification and somehow respond, and “erasers,” to remove the modification. For example, the PTM called histone acetylation, which functions to regulate transcription by making histones associate more or less strongly with DNA, uses histone acetyltransferases as writers, histone deacetylases as erasers, and bromodomains as readers (Xu et al., 2017). For the previously-mentioned PTM ADP-ribosylation, the writers are known as PARP domains (Li & Chen et al, 2014). There exist several classes of readers of ADP-ribosylation, including PAR-binding zinc fingers, PAR-binding linear motifs, WWE domains, and macrodomains;

this final class, the macrodomains, have also been found to remove ADP-ribosylation, thus functioning as erasers as well as readers of ADP-ribosylation (Barkauskaite et al., 2013).

In addition to its established housekeeping functions, evolutionary analysis of the PARP domains suggests an immunological role for ADP-ribosylation. As a conflict between a pathogen species and its host progresses over evolutionary time, each species evolves mechanisms to either increase its ability harm the other, or to neutralize some mechanism that the other organism uses to harm it (Daugherty et al., 2014). For example, the human protein APOBEC3G is able to prevent replication of HIV-1 if the virally encoded gene Vif is silenced; however, over the course of normal HIV-1 infection, the Vif protein antagonizes APOBEC3G such that the virus is able to replicate (Ran et al., 2016). These molecular arms races leave an identifiable gene fingerprint, in the form of rapidly evolving gene segments (Daugherty et al., 2014). The PARP domains involved in housekeeping functions have not been found to be evolving rapidly; this is to be expected, as any mutation in these proteins would likely reduce the fitness of the organism, and reduce the probability of the mutation propagating among the species (Daugherty et al., 2014). However, genomic analyses between various primate species have identified a subset of PARP domains, specifically PARP4, PARP9, PARP13, PARP14, and PARP15, as rapidly evolving (Daugherty et al., 2014). In fact, some of these rapidly-evolving PARPs have already been shown to affect host-pathogen interactions. For example, overexpression of PARP13 has been found to inhibit replication of viruses from various families, including a hepadnavirus, a togavirus, multiple filoviruses, and a retrovirus (Bick et al., 2003; Gao, Guo, & Goff, 2002; Mao et al., 2013; Muller et al., 2007). In addition, PARP4 has been confirmed to be expressed in certain innate immune cells (Berger et al., 2009). Thus, although much more research into the functions of PARP13 and

PARP4 is needed, they provide evidence that there is indeed a correlation between rapid evolution and participation in host-pathogen conflicts.

Additional evidence for an immunological role for ADP-ribosylation can be found in research into viral macrodomains. The nsP3 macrodomain, encoded by the Sindbis virus, has been shown to be essential for success of the virus (Park & Griffin, 2009). Mutation of single amino acid residues in this macrodomain were found to inhibit the ability of the virus to replicate, kill mature neurons, and cause pathology in mice. (Park & Griffin, 2009). In addition to Sindbis virus, macrodomains have been identified in several other families of positive sense RNA viruses, including medically relevant viruses such as Hepatitis E virus and the rubella virus (Gorbalenya et al., 1991; Park & Griffin, 2009). These macrodomains are often found closely associated to viral proteases, which frequently antagonize host proteins in addition to their role in the viral life cycle; however, no evidence exists to connect these two functions (Morazzani et al., 2019; Park & Griffin, 2009). Additionally, most viral macrodomains have been found to cleave ADP-ribose; thus, the mechanism of host antagonism by these macrodomains has been proposed to be cleavage of ADP-ribosylation involved in antiviral responses (Li et al., 2016). Considering that viruses encode mechanisms to interact with host ADP-ribosylation, it is likely that this system plays some role in antiviral defenses.

Returning to the rapidly evolving members of the PARP family, the PARPs PARP9, PARP14, and PARP15 share a very interesting feature: they all contain macrodomains, in addition to PARP domains. These three proteins, known as the macro-PARPs, are the only identified human proteins which contain a macrodomain and a PARP domain and are the only known human proteins which contain more than a single macrodomain (Daugherty et al.,

2014). The function of PARP15 is generally poorly understood; one study found a correlation between certain polymorphisms in PARP15 and survival rate of acute myeloid leukemia, but little other literature exists on it (Lee et al, 2016). Additionally, one study found PARP9 to play a role in the development of diffuse large B-cell lymphoma; another found PARP9 to increase interferon efficacy and antagonize a viral protease, both for the purpose of fighting viral infection (Camicia et al., 2013; Zhang et al, 2015). Several studies into PARP14 have also found it to be involved in the signaling pathways of the immune signaling molecule IL-4, thereby implicating it in the development of certain B cell lymphomas (Cho et al., 2009; Mehrotra et al., 2010). Finally, one study found that PARP14 and PARP9 function antagonistically to each other to control macrophage activation by regulating downstream signaling of the IL-4 ligand (Iwata et al., 2016). These immune-related functions for PARP14 and PARP9 are consistent with their observed rapid rate of evolution; however, more research into these proteins is needed to clarify their role in host-pathogen interactions.

Past research took steps to characterize the nature of ADP-ribose binding by macrodomains. Sequence alignment of various human and viral macrodomains has revealed a ligand-binding pocket shared by many otherwise structurally-diverse macrodomains; structural analysis and binding affinity assays have found these ligand-binding pockets to bind to ADP-ribose with high affinity (Daugherty et al., 2014; Karras et al., 2005). Some evidence of specificity of macrodomain binding, beyond a general affinity to ADP-ribose, does exist, in that the number of ADP-ribose subunits attached to the target protein seems to affect the ability of different macrodomains to bind to ADP-ribose. For example, the three macrodomains of PARP14 have been shown to selectively bind single ADP-ribose subunits, called mono-ADP-ribosylation (MARylation), whereas the histone macrodomain

macroH2A1.1 binds long, branching chains of ADP-ribose subunits called poly-ADP-ribosylation (PARylation) (Aguilera-Gomez et al., 2016; Forst et al., 2013; Timinszky et al., 2009). In a study of cellular stress responses to amino acid formation, these two macrodomains (or groups of macrodomains) were found to localize differently in cells under the same conditions; this is consistent with differential binding capabilities of the two macrodomains to MARYlation and PARylation (Aguilera-Gomez et al., 2016). Additionally, this same study found that none of the macrodomains from PARP14 are individually able to bind mono-ADP-ribosylation, suggesting that the three macrodomains work in conjunction to mediate this affinity to MARYlation (Aguilera-Gomez et al., 2016). This differential binding ability based on number of ADP-ribose subunits shows that specificity in macrodomain binding, beyond a nonspecific affinity for ADP-ribose, is possible.

Another possibility for specificity of ADP-ribose binding by macrodomains is sequence specificity; that is, macrodomains binding to ADP-ribosylated residues differently depending on the amino acid residues adjacent to the site of modification. Other PTMs have been shown to utilize sequence specificity to control their reader domains' binding ability; an example of this is the phosphorylation system, which participates in regulation of cell division and differentiation, among other roles (Pawson & Gish, 1992). One type of reader domain for this system are the SH2 domains of receptor tyrosine kinases (RTKs), which bind to phosphorylated tyrosine residues; these domains show sequence specificity, meaning that the ability of the domain to bind depends on the amino acid residues adjacent to the phosphorylated tyrosine being read (Zhou et al., 1993). Additionally, the SH2 domains of different RTKs have been found to show different sequence specificities, and further research

has shown these differences to meaningfully impact the functions of these proteins (Colicelli, 2010; Zhou et al., 1993).

This question of macrodomain sequence specificity does not seem to be a widely-asked question, and little existing research seems to take this possibility into consideration. For example, one study done by Dani et al. uses the archaeal macrodomain Af1521 in experiments to identify ADP-ribosylated proteins in cells (Dani et al., 2009). The Af1521 macrodomain, originating from the archaea *Archaeoglobus fulgidus*, was the first macrodomain proven to bind to ADP-ribose; the study that presented this data identified affinity for ADP-ribose as a shared feature of macrodomains and raised the possibility of different macrodomains having different specificities to either MARYlation or PARYlation (Karras et al., 2004). In fact, Dani et al. show that the Af1521 macrodomain can bind to both PARYlation and MARYlation, but do not raise the possibility of sequence specificity in its ADP-ribose binding (Dani et al., 2009). Any experiment that takes advantage of the high affinity of macrodomains to ADP-ribose could be affected by unidentified sequence specificity; thus, resolution of this question is crucial to future research into ADP-ribosylation.

Experimentation to address the issue of sequence specificity in ADP-ribose binding must address a central question: do structurally unique ADP-ribose binding domains, which bind to the same number of ADP-ribose subunits (i.e. MARYlation or PARYlation), bind to different ADP-ribosylated proteins? The macrodomains seem to be a good set of ADP-ribose binding domains with which to investigate this question: although they are very structurally diverse, structural analysis of their shared ligand-binding pocket has found that they are only capable of binding to the terminal ADP-ribose subunit in a chain of ADP-ribose subunits,

meaning that every macrodomain is capable of recognizing MARylation or PARylation (Teloni & Altmeyer, 2016). Thus, any evidence of two macrodomains binding to different proteins under the same cellular conditions would open up the possibility of ADP-ribose binding being sequence specific. Additionally, considering that the macro-PARPs have been found to be rapidly evolving, investigation of their macrodomains binding in the context of immunologically-relevant cell conditions (such as viral infection, exposure to interferon, or exposure to the dsRNA-mimicking molecule poly (I:C)) may produce interesting results; thus, they are good candidates for use in experimentation (Daugherty et al., 2014).

One experiment that could produce this evidence of differential binding is investigation of the localization of macrodomains under different cellular conditions. If cells are made to express constructs consisting of a macrodomain fused to a fluorescent protein, then the localization of the macrodomain, presumably driven by its binding to ADP-ribose, can be tracked by fluorescence microscopy (Aguilera-Gomez et al., 2016). Any fluorescence pattern that is produced under different cellular conditions can be compared between macrodomains, to look for differences. In addition to the immunological signals described previously, sodium arsenite exposure could also be utilized in these experiments. Cells produce structures known as stress granules in response to arsenite exposure; ADP-ribosylation is an integral part of the formation of these stress granules, and past experiments have shown that certain macrodomains localize to stress granules (Aguilera-Gomez et al., 2016; Leung et al., 2011). Cells expressing constructs with different macrodomains can be exposed to sodium arsenite, and the ability of the different macrodomains to localize to the stress granules can be observed. Any difference in this ability would suggest differences in ADP-ribose binding by the macrodomains.

This kind of experiment has some inherent flaws, however. First and foremost, localization of these proteins may be influenced by factors other than binding to ADP-ribose. For example, larger constructs may be excluded from the nucleus due to their size (Wang & Brattain, 2007). Additionally, if any of the constructs contain a nuclear localization signal, then a change in localization independent of binding to ADP-ribose may be observed. For any results from these localization experiments, these alternative explanations must be ruled out before any conclusions about sequence specificity can be made.

The procedure outlined in Dani et al. presents a more direct way to address the question of macrodomain binding specificity. A macrodomain can be fused to some purifiable tag, the fusion construct can be expressed inside a cell, and then the tag can be isolated; any proteins bound to the macrodomain would be pulled down as well, and these proteins can be identified by mass spectrometry (Dani et al., 2009). As these proteins would be pulled down because of the affinity of the macrodomain to an ADP-ribose modification, the identity of the proteins pulled down would rely on the binding affinity of the macrodomain; thus, if this experiment was repeated with different macrodomains and different proteins were pulled down by the different macrodomains, then that would suggest that the different macrodomains bind to ADP-ribose with sequence specificity. Additionally, as this experiment would be carried out *in vitro* under more tightly controlled conditions than the localization experiments, there would be less opportunity for confounding factors to affect the results.

MATERIALS AND METHODS:

NI-NTA RESIN PROTEIN PURIFICATION:

All procedures were performed at 4°C, to minimize spontaneous ADP-ribose hydrolysis. BL21 *E. coli* cells were transformed with the pAR041 plasmid (Fig. 1). This plasmid consists of a pET28b backbone with the archaeal-origin macrodomain Af1521 cloned to the C-terminus. The pET28b backbone expresses the desired insert, in this case Af1521, with six additional histidine residues on the N-terminus, composing a 6xHis tag. Expression of this product is under control of the lac operon promoter and repressor, allowing for activation of expression upon exposure to the lactose mimic IPTG. These transformed *E. coli* were grown to approximately OD 1.0, and 1:1000 IPTG by mass was added to the culture; the cells were left to express the 6xHis-Af1521 construct overnight.

Following this, the cells were lysed via incubation with lysozyme and subsequent sonication, and Nickel-NTA (Ni-NTA) resin (kept at 4°C) was incubated with the resulting lysate for 1 hour. The resin was then washed to remove any non-bound protein. Next, mammalian cells were lysed via incubation in a hypotonic buffer for 40 minutes, and the Ni-NTA resin with bound 6xHis-Af1521 fusion protein was incubated with the resulting lysate. The lysate was let incubate at least 1 hour, such that any ADP-ribosylated proteins had ample opportunity bind to the Af1521 macrodomain. The resin was then washed again to remove any non-bound protein. One of two different elution procedures were then performed. The first, incubation with only 500mM imidazole for 15 minutes to compete with histidine for binding to the nickel column, thus eluting the entire Af1521-ADP-ribosylated protein complex; the second, incubation with 0.5M hydroxylamine for 15 minutes to hydrolyze ADP-ribose from aspartate and glutamate residues and thus elute the formerly ADP-ribosylated

protein, followed by incubation with 500mM imidazole for 15 minutes to elute any remaining protein. Samples taken at each step, and gel electrophoresis used for analysis.

LOCALIZATION OBSERVATION VIA TRANSIENT TRANSFECTION OF PLASMID:

Plasmids for all localization experiments used the pDL2259 backbone (Fig. 7). This backbone expresses any desired insert with an HA tag and the fluorescent protein mCherry fused at the N-terminus. This vector is expressed in mammalian cells; additionally, this plasmid allows for generation of cell lines that produce the mCherry fusion product at stable levels upon doxycycline induction; generation of these cell lines is described in further detail in the relevant section.

Twenty-four hours before performing transfection, Huh7 cells were split into a 24-well dish. Transfections were performed when cells at ~50-60% confluency. Between 100 and 500ng of plasmid with pDL2259 backbone was added to 100µl room temperature Thermo Fisher Scientific Opti-MEM reduced media. Solutions were mixed well, and incubated at room temperature for 5 minutes. Following this, 1.5µl room temperature Mirus Bio TransIT Transfection Reagent was added, mixed well, and incubated at room temperature for 15 minutes. Finally, the mixture was added dropwise onto wells, the plate was rotated to mix, and cells were incubated at 37°C. Cells were imaged 24 hours after transfection. To image cells, the whole well was examined and images were taken that are representative of the whole well.

To induce cells with Interferon Beta or Gamma, either 100 units/mL (for Gamma) or 1000 units/mL (for Beta) was added to the well around 6 hours post-transfection. Cells were visualized 24 hours post-transfection, as was done with other conditions.

LOCALIZATION OBSERVATION VIA DOXYCYCLINE INDUCTION:

U2OS cell lines stably expressing different mCherry-macrodomain fusion products, inducible by exposure to doxycycline, were generated. To do this, U2OS cells were cotransfected with a donor plasmid in the pDL2259 backbone (Fig. 7) and the pOG44 plasmid, encoding a recombinase. The recombinase replaces a specific site in the U2OS cell genome with a portion of the donor plasmid, including the region encoding the protein of interest and the region encoding resistance to the antibiotic hygromycin; cells that underwent a successful recombination event are selected for by growing the cells with hygromycin. The resulting cells will express the protein of interest upon induction by a different antibiotic, doxycycline.

24 hours before induction, cells were split into a 24-well dish. When the cells were ~50-60% confluent, 1000ng/mL doxycycline was added to the well. Cells were visualized 24 hours after induction. To induce cells with Interferon Beta or Gamma, either 100 units/mL or 1000 units/mL Interferon was added to the well 8 hours post-induction. To expose cells to Poly (I:C), Poly (I:C) was first combined with lipofectamine, allowing the molecule to enter the cells. Either 10 ng/mL or 1 ng/mL Poly (I:C) was then added to the well 8 hours post-induction. To infect cells with virus, Sindbis virus was introduced to the well at approximately MOI 10 or MOI 1, 8 hours post-induction. For Interferon, Poly (I:C), and viral infection experiments, cells were visualized 24 hours post-induction. Finally, to observe the effects of sodium arsenite exposure, either 5mM or 0.5mM sodium arsenite was added to the well 8 hours after induction, and the resulting localization was observed 30 minutes, 60 minutes, and 90 minutes post-addition.

RESULTS:

PULLDOWN EXPERIMENTS:

When performing these experiments, two different elution methods were utilized to liberate proteins bound to the column construct. The first, imidazole, is structurally quite similar to histidine; thus, imidazole is introduced at a concentration sufficient to outcompete the histidine tag, which is fused to the macrodomain, in its binding to the nickel column (Bornhorst & Falke, 2000). The entire construct is therefore separated from the nickel column. The other elution method used, hydroxylamine, has been shown to cleave ADP-ribose from modified aspartate and glutamate residues (Vivelo & Leung, 2014). Through this activity, hydroxylamine frees a subset of proteins (depending on the identity of the modified residue) from the construct. A control was also put in place for this elution: each pull-down experiment was run in duplicate, such that the experiment in question was repeated simultaneously with the human lysate being pretreated with hydroxylamine (at the same concentration as the elution step). Any hydroxylamine-pretreated condition should thus show no protein being eluted by the hydroxylamine elution.

In order to construct a system to isolate ADP-ribosylated proteins, the ability of 6xHis-tagged macrodomains to be purified were first assessed. One control that was put in place was to process the lysate of a bacterial culture that was not induced to produce the construct; however, in the SDS-PAGE gel analyzing this experiment, the lanes for the sample using uninduced bacterial lysate shows that the protein was still expressed, indicating some failure of the lac operon repressor (Fig. 2). One possibility is that the lacI promoter failed to activate expression of the lacI repressor; thus, the 6xHis-Af1521 construct was able to be expressed freely (Fig. 1). The nickel column was able to bind to the 6xHis tag on the construct

effectively, as the construct is absent from the flowthrough lanes. Additionally, the imidazole elution was shown to be effective in removing the protein from the column, as there is a large amount of the protein present in the elution lanes.

The second portion of the system, whereby Ni-NTA column with Af1521 construct bound was incubated with human lysate to bind ADP-ribosylated proteins, was less successful. Initial experiments showed that this procedure could purify PARP10, a protein known to auto-ADP-ribosylate (Fig. 3; Yu et al., 2005). In order to assess the efficacy of the hydroxylamine elution, a purification was done where hydroxylamine was present for the entire procedure. The lack of any band in the “+ hydroxylamine elution” lane confirms that hydroxylamine can elute some ADP-ribosylation (Fig. 3). Additionally, although a small amount of PARP10 failed to bind to the column (as shown in flowthrough lanes), a large amount of it did bind, and was only removed by the final elution. This result confirms that this system could be used to purify ADP-ribosylated proteins.

The next experiment done to further refine this system was to identify any proteins in the bacterial and human lysates, other than 6xHis-Af1521, that could bind to the nickel column directly. A column was incubated with bacterial lysate whereby the culture had not been induced to produce the 6xHis-Af1521 protein and eluted; simultaneously, a column was incubated with the human lysate alone and eluted. Additionally, a column was incubated with the uninduced bacterial lysate followed by the human lysate and then eluted, as well as neither lysate. Finally, any purification with the human lysate was done in duplicate, with one copy being pretreated in hydroxylamine and the other not. Some of the samples of these procedures were ran on a gel and silver stained (Fig. 4). Lanes 7 and 13 on this gel show the different bacterial proteins that are capable of binding to a nickel column (Fig. 4). The large number of

bands in these lanes indicates that many bacterial proteins can bind to nickel. Similarly, lane 11 shows the different human proteins that can bind to a nickel column. For some reason, the imidazole elution of human lysate run over the column with no hydroxylamine pretreatment was not included in this silver stain; however, lane 11 and 16 can approximate this condition, as lane 17 would be equivalent to these two lanes combined together. Lane 11 seems to have no bands, and lane 16 seems to only have 2 bands (Fig. 4). These results suggest that relatively few human proteins can bind directly to the nickel column.

Following this result was an experiment to see if PARP10 is capable of binding to the nickel column in the absence of the macrodomain-containing construct. Four purifications were carried out simultaneously: two with the bacterial culture induced to produce the macrodomain-containing construct, and two with the culture not induced. Within each of these, one was treated with the human lysate pretreated with hydroxylamine, and one with the human lysate untreated. A Western blot of this experiment shows that the amount of PARP10 eluted in all four conditions seems to be the same (Fig. 5A). This result indicates that PARP10 was not preferentially bound to the macrodomain. The same blot was then stripped and reprobed for the macrodomain-containing construct. The resulting large bands in lanes 8 and 9 show that there was in fact a large amount of the macrodomain present in those conditions (Fig. 5B). Thus, the macrodomain was unable to bind to PARP10.

A new experiment was then carried out, using new 293T cell pellets transfected to express PARP10, to determine if an uninduced bacterial lysate, and thus not expressing the macrodomain of interest, could purify the PARP10 protein. Note that, in the blot analyzing these experiments, no PARP10 is present in any of the elution lanes, and the amount of PARP10 in the flowthrough lanes is approximately equal to that of the original lysates (Fig.

6). These results show that PARP10 was again unable to bind to the macrodomain construct. These experiments are certainly worth future pursuit, but from this point my focus switched to the localization experiments.

LOCALIZATION EXPERIMENTS:

Initial localization experiments were done by transiently transfecting Huh7 cells such that they would express fluorescently-tagged macrodomains, and observing the pattern of fluorescence within the cells 24hrs post-transfection. In total, 19 plasmids with the pDL2259 backbone were transfected in this way (Table 1). Initial experiments were done with the two single macros, SinV and Af1521, as well as the complete set of macros from PARP14, PARP15, and PARP9, and the empty vector as a negative control. These early data are not included here, as these constructs were imaged in higher quality later. Of these, all but one seemed to look like the empty vector negative control, which seemed to spread diffusely around the cells; the one exception was the construct with the three macrodomains of PARP14, which showed exclusion from the nucleus (Fig. 8).

Nuclear exclusion can be a result of a protein being too large to diffuse into the nucleus. Thus, to investigate this phenotype and identify its mechanism, constructs containing different combinations of the three PARP14 macros were produced and tested. Every construct containing the second of the three macros showed this phenotype of nuclear exclusion, suggesting that the phenotype is mediated by macro 2 (Fig. 9). In addition, each of these constructs containing macro 2 was mutated such that the 188th amino acid changed from a neutral glycine to a negatively charged glutamic acid, in the hopes that such a mutation would interfere with the ligand binding pocket of the macrodomain. However, no change in localization was observed with these mutations, and so those data are not included here. Every

construct tested by transient transfection was also transfected into cells that were later exposed to either Interferon Beta or Gamma, as well as Huh7 cells with the protein PARP13 knocked out (Table 1). However, these conditions seemed to make no difference in the observed localization of the constructs, and thus those data are not included here.

Moving forward, seven of these constructs were selected for creation of U2OS lines expressing the construct at more consistent levels (Table 2). Past observations regarding localization of the three macros of PARP14 and its G188E mutant, as well as the two macros of PARP9 and the SinV macro, were confirmed; closer inspection suggested that the Af1521 macro and the two macros of PARP15 were capable of localizing to the nuclei of the cells (Fig. 8). These cell lines were then exposed to varying levels of Interferon Beta, Interferon Gamma, and Poly (I:C); similarly to prior experiments, these conditions did not change the observed localization pattern, and thus those data are not included here. Additionally, these lines were exposed to differing amounts of sodium arsenite, and then visualized after 30 minutes, 60 minutes, and 90 minutes. Every construct containing a macrodomain, except for those from PARP15, showed localization to small points in some number of cells in the time between addition of sodium arsenite and cell death; existing literature suggests that these small points are stress granules, although further experimentation is needed to confirm this identification (Fig. 10; Aguilera-Gomez et al., 2016). Finally, these cells were infected with Sindbis virus at MOI ~10 and MOI ~1, but no change in localization pattern was observed; again, those data are not included here.

DISCUSSION:

Attempts to utilize a Ni-NTA-macrodomain-ADP-ribose binding system to purify ADP-ribosylated proteins proved unsuccessful. This system is capable of purifying ADP-ribosylated proteins; although some PARP10 was present in the flowthrough, indicating that it did not bind to the column, a significant portion of the PARP10 in the sample was able to bind to the column, was not removed by the washes, and was only removed by the final elution (Fig. 3). For this system to be used to identify ADP-ribosylated proteins, every modified protein in the sample cell lysate must show this same behavior. In addition, many different bacterial and human proteins can bind to the column; they may be able to do so because they, by chance, have several His residues in succession, which can bind to nickel (Fig. 4). If this system were to be used to identify ADP-ribosylated proteins, then proper controls must be run such that all human and bacterial proteins that bind to nickel independently of the macrodomain can be identified. These proteins could then be eliminated from the list of proteins generated by any mass spectrometric analysis.

In the first experiment where PARP10 was unable to bind to the column, there are faint bands present in the elution lanes; they are likely present because the column was not washed sufficiently before elution (Fig. 5A). The fact that the four bands are equal in intensity suggests that they were not purified by the system; thus PARP10 remained present, although unbound, in the solution that the column was suspended in. The fact that the macrodomain was eluted by imidazole indicates that the problem was with PARP10 binding to the macrodomain, rather than the macrodomain binding to the nickel (Fig. 5B) Further experiments yielded similar results: the amount of PARP10 present in the lysate is the same as the flowthrough, indicating that no PARP10 bound to the column (Fig. 6). One explanation

for the sudden extinction of binding by PARP10 to the macrodomain is that PARP10 may not have been able to automodify in these cells. ADP-ribosylation requires NAD⁺ as a substrate; it is possible that there was not sufficient NAD⁺ in the cells for the PARP10 to automodify (Jankevicius et al., 2013).

The data shown here does not help to address the question of differential ADP-ribose binding by macrodomains. However, considering that this system was shown to pulldown an ADP-ribosylated protein, further refinement and testing may allow this system may be able to shed light on the issue (Fig. 3). In order to minimize off-target binding, wash conditions must be calibrated to remove any weakly-bound proteins without removing proteins bound to the macrodomain via ADP-ribose. In addition, it must be proven that the system always binds to ADP-ribosylated proteins; PARP10 might be an effective positive control to determine this, although further experimentation is needed. Additionally, no non-ADP-ribosylated proteins must be pulled down by the system. Silver stain, and other protein staining systems, seems to be a good way to assess this. Additionally, a mutant PARP10 which is unable to automodify could be used as a negative control in these experiments. If these controls were shown to function as expected, then different 6xHis-tagged macrodomains could be used instead of Af1521, and the proteins identified by mass spectrometric analysis could be compared. Differences in the proteins pulled down by each macrodomain would suggest that different macrodomains do in fact selectively bind to certain ADP-ribosylated residues, and not others. On the other hand, a result of each macrodomain pulling down the same proteins would suggest that macrodomains bind to ADP-ribose indiscriminately.

The localization experiments, in contrast, may be able to address the question of differential binding of ADP-ribose by macrodomains. Three broad classes of localization

phenotype were observed: no localization, shown by the SinV macro and the two macros of PARP9, nuclear exclusion, shown by the three macros of PARP14, and nuclear localization, shown by the Af1521 macro and the two macros of PARP15 (Fig. 8). These differences in localization suggest that each set of macros may bind to ADP-ribose differently; however, several factors that can alter protein localization, including cellular trafficking, nuclear localization signals, and protein size, must be addressed before this conclusion can be made. Regarding the first factor, addition of the mCherry negative control shows that normal protein trafficking does not lead to any observed nuclear exclusion or localization. In addition, amino acid sequences called nuclear localization signals can signal importins on the nuclear pore to either import the protein into the nucleus or export it from the nucleus (Lange et al., 2006). Analysis of the amino acid sequence of every construct tested found that none contained nuclear localization signals, thus discounting this explanation.

Finally, there is a limit to the size of proteins that can freely diffuse through nuclear pores. Conventional wisdom suggests that proteins with a molecular weight larger than 60kDa are excluded from the nucleus, although recent research found that proteins as large as 100kDa are capable of diffusing into the nucleus; regardless, at 92kDa, the PARP14 3 macros construct is near enough to this limit that molecular weight must be disproven as the reason for its observed nuclear exclusion (Wang & Brattain, 2007). To address this issue, different combinations of the three macros of PARP14 were cloned into the construct, and the localizations of each construct were observed; these experiments showed that any construct containing the second macro of PARP14 is excluded from the nucleus (Fig. 9). The smallest of these nuclear-excluded constructs, the one containing macro 2 of PARP14 alone, has a molecular weight of 52kDa, far smaller than any proven nuclear diffusion limit (Wang &

Brattain, 2007). Thus, the observed nuclear exclusion of the PARP14 3 macros construct does not seem to be a consequence of its size.

Another line of inquiry into this second macro of PARP14 was also pursued: past studies have shown that a single glycine residue in the ligand-binding pocket of every macrodomain mediates its ability to bind to ADP-ribose (Aguilera-Gomez et al., 2016). For every construct containing the second macro of PARP14, its G188E mutant counterpart was generated and tested, with the expectation that this mutation from a neutral residue to a negative residue would prevent binding to ADP-ribose and thus lead to extinction of the nuclear-exclusion phenotype. However, this result was not observed (these data are not included, as they localize the same as their wild type counterparts). Future experimentation may reveal why this mutation was not observed to disrupt ADP-ribose binding.

Attempts to alter localization of these constructs by exposing the cells to various immunological signals were largely unsuccessful. Cells were exposed with Interferon Beta, Interferon Gamma, and Poly (I:C), and were infected with Sindbis virus; however, no change in localization of any macrodomain construct was observed in response to any of these signals. These experiments were pursued in response to the evolutionary data suggesting a role for ADP-ribosylation and macrodomain-containing proteins in host-pathogen interactions, as well as the observed role of the nsP3 macrodomain in Sindbis virus infection (Daugherty et al., 2014; Park & Griffin, 2009). The data presented here are not necessarily incompatible with this suggested role of ADP-ribosylation. It is possible that this system of visually identifying changes in localization of fluorescent proteins is simply not sensitive enough to identify alterations in ADP-ribosylation within the cell. For example, if proteins were newly ADP-ribosylated in response to interferon exposure, but these proteins are

localized in the same cellular compartment as the modified proteins in the cell under normal conditions, then no change would be observed in these experiments. Further inquiry to identify such changes would be best served by a procedure to isolate and identify ADP-ribosylated proteins; in fact, the construct utilized in these experiments contains an HA tag that could be used in this way. The proteins that are pulled down by purification of these HA-tagged proteins can be identified, and compared between the different macrodomains. Any difference in the proteins identified would suggest that these proteins bind to ADP-ribose differently.

Experiments with sodium arsenite exposure, in contrast to those utilizing immunological signals, were more successful in altering the phenotypes observed in these cells: in every cell line tested, except for those expressing the construct containing the human PARP15 protein, sodium arsenite exposure led to generation of bright spots of fluorescence in the cells (Fig. 10). Past experiments utilizing macrodomains fused to fluorescent proteins found that the macrodomains of PARP14 localized to small points in the cell, and that the stress granule-binding protein FMR1 also localized to these small points; this colocalization proved that the PARP14 macrodomains could localize to stress granules (Aguilera-Gomez et al., 2016). Thus, as replication of those experiments produced similar fluorescence patterns here, it is possible that the spots observed here are indeed stress granules (Fig. 10). However, there are several further experiments that must be done to confirm this: in particular, these fluorescence patterns must be shown to colocalize to stress granules. This is important to prove because protein aggregates, which constitute much of the mass of stress granules, have been shown to autofluoresce; thus, it is possible that the spots observed in these experiments are merely protein aggregates autofluorescing (Aguilera-Gomez et al., 2016; Schlick et al.,

2009). This possibility must be ruled out before any conclusions can be drawn from the data presented here.

One final factor relevant for any investigation into the binding of ADP-ribose by macrodomains is the observed ability of some macrodomains to cleave ADP-ribose residues. In fact, the first macrodomain of PARP14, the macrodomain encoded by the Sindbis virus, and the archaeal macrodomain Af1521, which were all utilized in these experiments, show ADP-ribosylhydrolase activity (Jankevicius et al., 2013). Further investigation is necessary to assess how this ADP-ribose cleaving activity has affected the results presented here; one potential way to go about this is to produce versions of these constructs with mutations to inactivate any ADP-ribose cleaving activity, repeat these experiments, and compare the results to the wild type versions to determine the effect, if any, that this cleaving activity had on the data shown here.

In total, the best evidence presented here suggests differential binding capabilities by different macrodomains. Various macrodomains were found to localize to different compartments within the cell, with some showing localization to the nucleus, others to the cytoplasm, and yet others showing no apparent preference in localization. Having ruled out the size of the proteins as a confounding factor and failed to identify any nuclear localization signals in these proteins, these data suggest that the difference in localization between these different macrodomains is a result of the difference in their ADP-ribose binding activities. In addition, preliminary data leaves open the possibility of the PARP15 macrodomains differing in their ability to localize to stress granules; however, more research must be done to conclusively prove this. The pulldown experiment described previously, if refined to be more

replicable, is likely the best approach going forward for addressing this question of differential ADP-ribose binding activity of macrodomains.

FIGURES AND TABLES:

Table 1: The full list of plasmids that were tested in all experiments utilizing transient transfection. These plasmids utilized the pDL2259 backbone, and thus expressed the indicated insert with an HA tag and the fluorescent protein mCherry fused to the N-terminus. These fusion products were expressed upon transfection into mammalian cells.

Plasmid Name	Insert
pDL2259	none
pDL2260	PARP14 3 macros
pDL2261	PARP9 2 macros
pDL2262	SinV (viral) single macro
pDL2263	PARP15 2 macros
pDL2279	Af1521 (archaeal) single macro
pDL2284	PARP14 macros 1+2
pDL2285	PARP14 macros 2+3
pDL2286	PARP14 macro 1
pDL2287	PARP14 macro 2
pDL2288	PARP15 macro 1
pDL2289	PARP15 macro 2
pDL2290	PARP9 macro 1
pDL2291	PARP9 macro 2
pDL2292	PARP14 macro 3
pDL2299	PARP14 macro 2, G188E mutant
pDL2300	PARP14 3 macros, macro 2 G188E mutant
pDL2301	PARP14 macros 1+2, macro 2 G188E mutant
pDL2302	PARP14 macros 2+3, macro 2 G188E mutant

Table 2: The full list of cell lines generated for use in experiments utilizing doxycycline induction. These cell lines were generated by recombination of plasmids utilizing the pDL2259 backbone with a portion of the cell genome. Doxycycline was then used to induce expression of constructs consisting of the indicated insert with an HA tag and mCherry fluorescent protein fused to the N-terminus.

Cell Line Stock Number	Insert
DH004	none
DH005	Af1521 (archaeal) single macro
DH006	SinV (viral) single macro
DH007	PARP14 3 macros
DH008	PARP14 3 macros, macro 2 G188E mutant
DH009	PARP15 2 macros
DH010	PARP9 2 macros

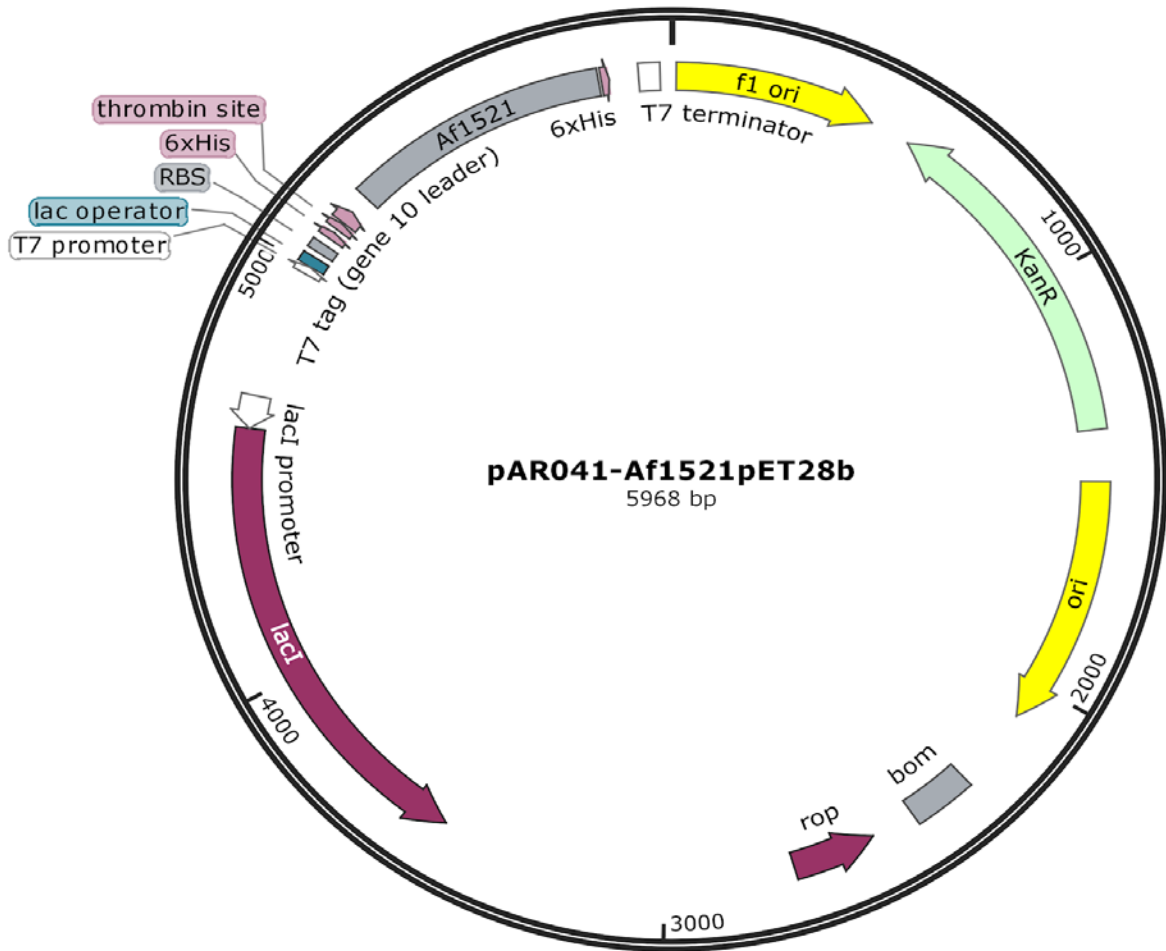


Figure 1: Expression vector pAR041, expressing Af1521 macrodomain with N-terminal 6xHis tag in *E. coli* (created via SnapGene). pET28b backbone includes transcriptional control via upstream lac operator, allowing activation of protein expression upon addition of lactose mimic IPTG. Kanamycin resistance (KanR) allows for selection of clones transfected with pAR041.

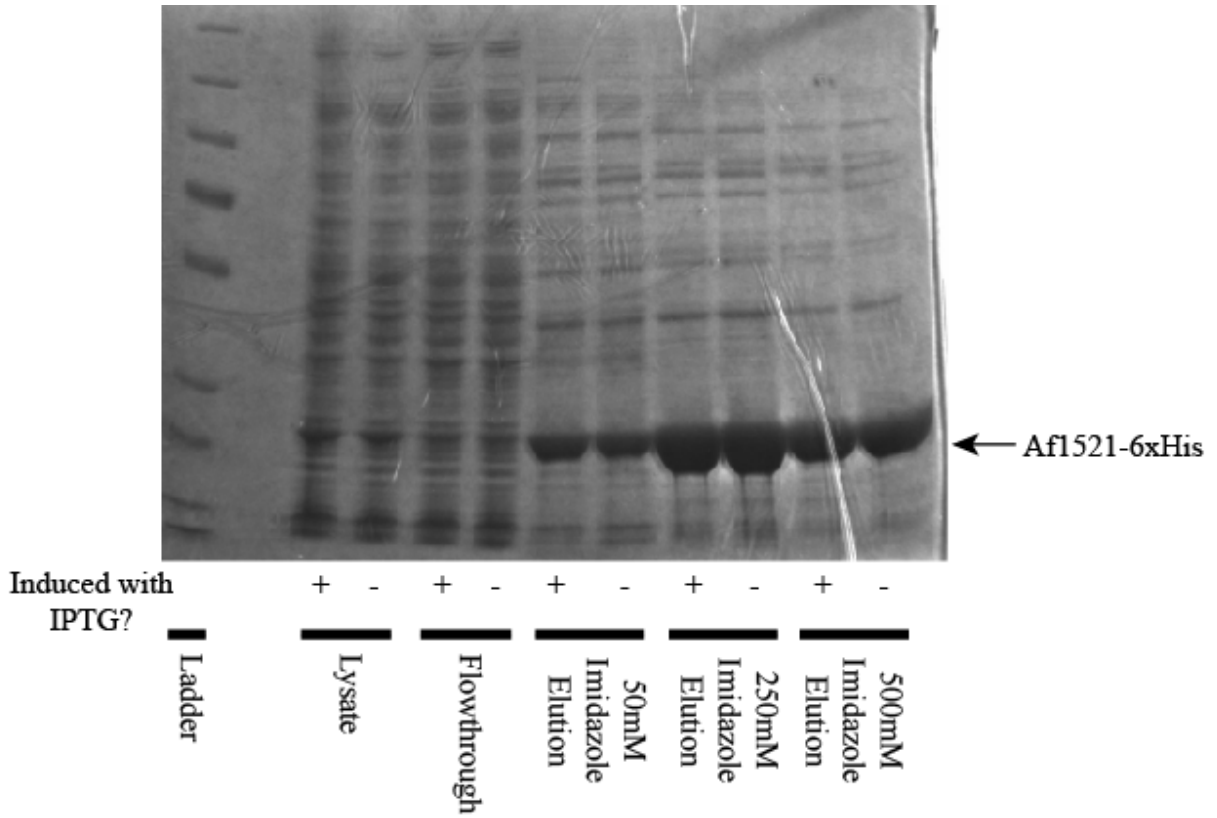


Figure 2: Coomassie stained SDS-PAGE gel showing binding of the 6xHis-Af1521 construct to the nickel column. Ni-NTA column was incubated for 1 hour with lysate from bacterial cells either induced to express 6xHis-Af1521 construct or uninduced, washed, and eluted by incubating with increasing concentrations of imidazole. PageRuler Plus protein ladder run in Lane 1.

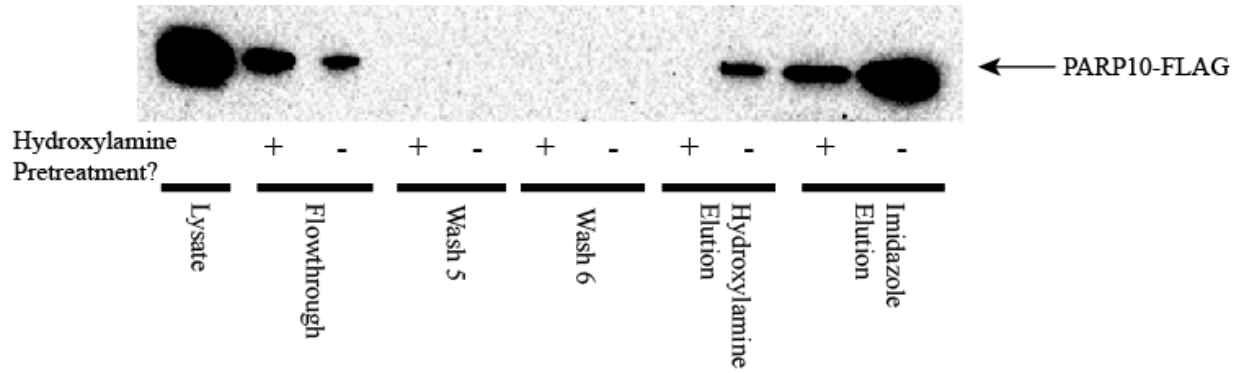


Figure 3: A Western blot probing for FLAG showing purification of PARP10-FLAG by Ni-NTA column with bound macrodomain. Ni-NTA column was incubated with bacterial lysate containing 6xHis-Af1521 construct, followed by incubation with human lysate expressing auto-modifying PARP10, and then elution with hydroxylamine and imidazole. Lanes marked “+” indicates that samples were incubated in hydroxylamine for the whole experiment.

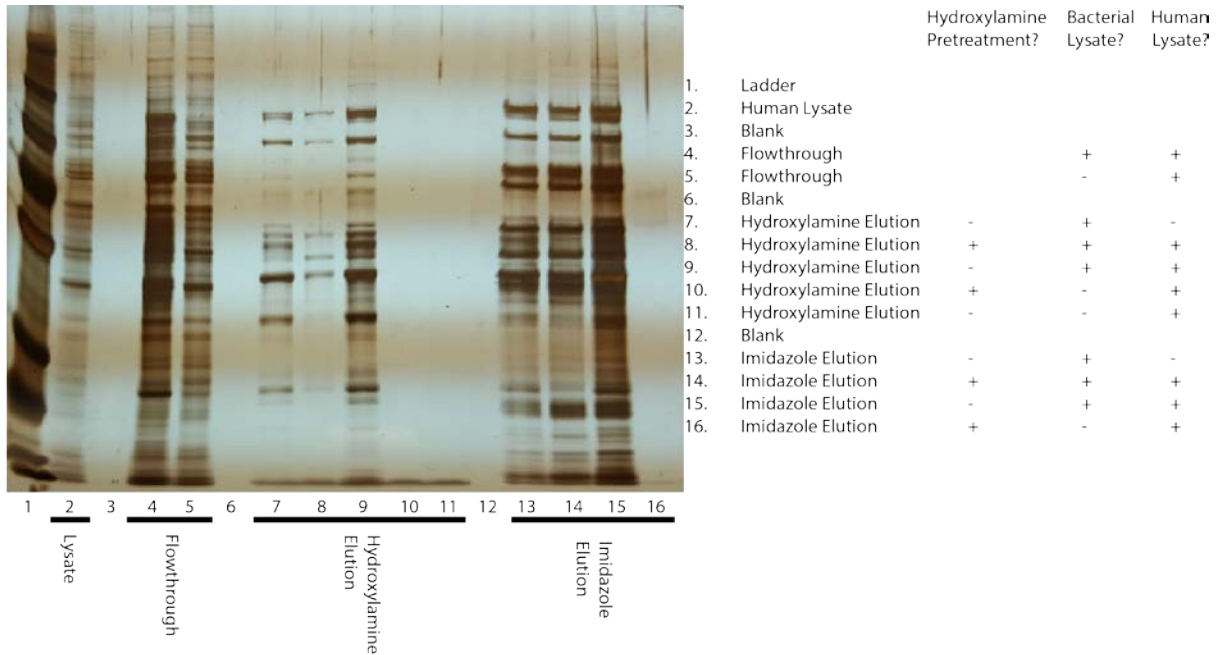


Figure 4: A silver stain of an SDS-PAGE gel showing various human and bacterial proteins binding to Ni-NTA column. Procedure to purify ADP-ribosylated proteins from human lysate was carried out, with multiple purifications being run in parallel; however, for each replication, different steps in the purification were omitted, and with some including a hydroxylamine pretreatment. In addition, no bacterial lysates were induced with IPTG. Silver stain reveals all proteins present in a gel.

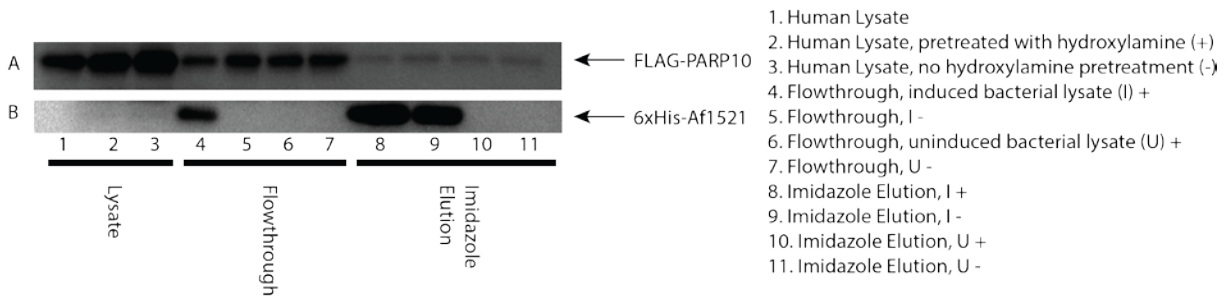


Figure 5: A Western blot probing for (A) FLAG and (B) 6xHis, showing the inability of FLAG-PARP10 to bind to the Ni-NTA column, despite the presence of the 6xHis-Af1521 macrodomain. Procedure to purify ADP-ribosylated proteins was carried out, with multiple purifications being run in parallel; however, some replications used bacterial lysate not induced to produce 6xHis-Af1521, and with some including a hydroxylamine pretreatment.

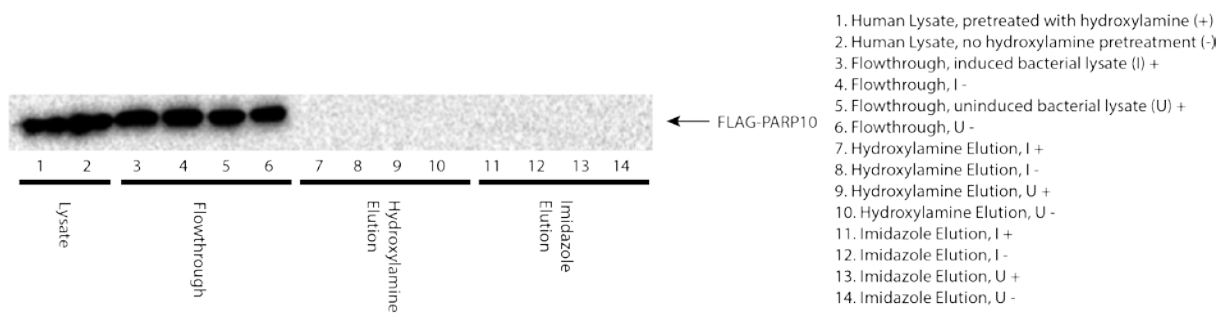


Figure 6: A Western blot for FLAG, showing the inability of FLAG-PARP10 to bind to the Ni-NTA column. Procedure to purify ADP-ribosylated proteins was carried out, with multiple purifications being run in parallel; however, some replications used bacterial lysate not induced to produce 6xHis-Af1521, and with some including a hydroxylamine pretreatment. This experiment was carried out to determine if an uninduced bacterial lysate could pulldown the PARP10 protein; however, note that the lysate and flowthrough lanes are equivalent, indicating that no FLAG-PARP10 bound to the column.

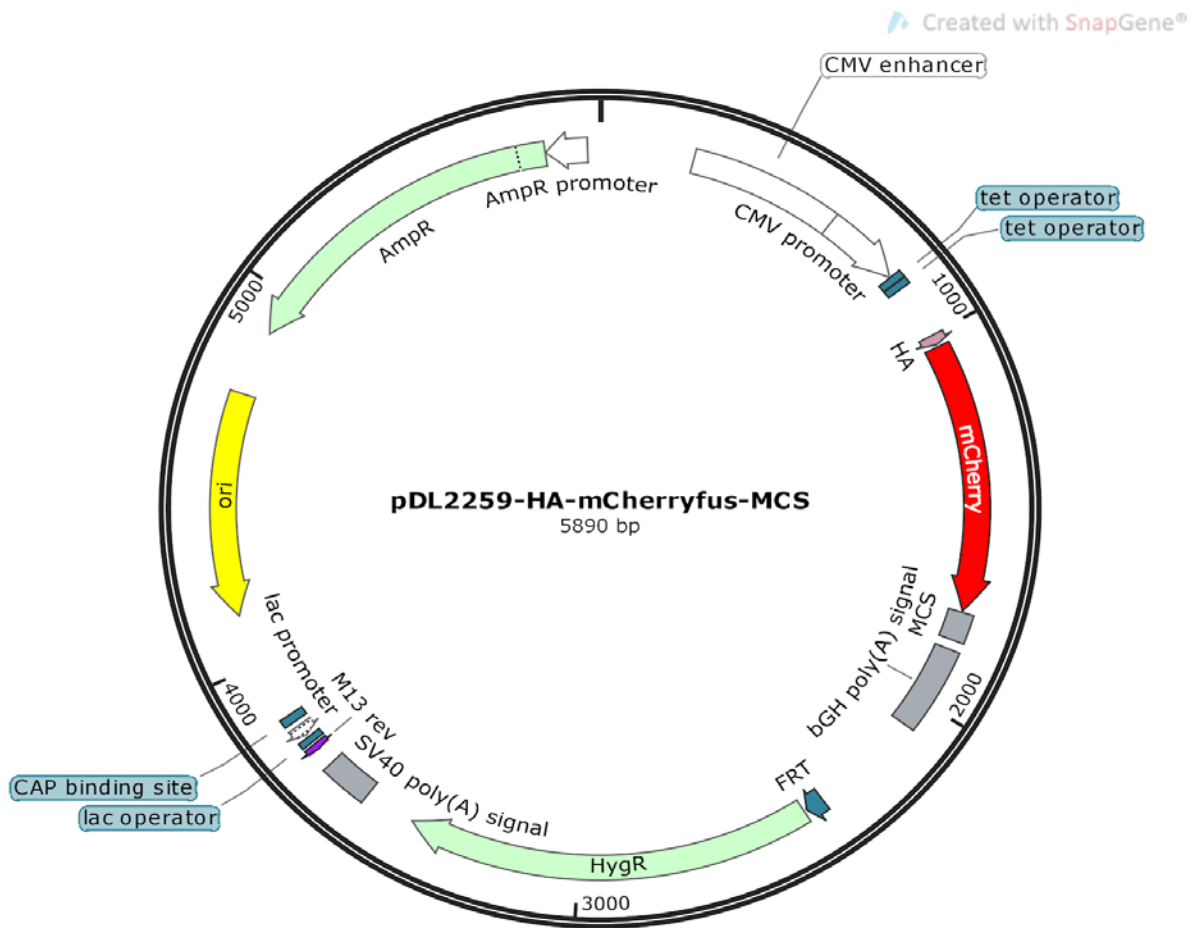


Figure 7: Expression vector pDL2259, expressing mCherry-macrodomein fusion proteins with N-terminal HA tag in human cells (created via SnapGene). pDL2259 backbone includes multiple cloning site (MCS) allowing for different macrodomains to be cloned into the construct. Plasmid can be introduced via transient transfection; additionally, hygromycin resistance (HygR) allows for generation of doxycycline-inducible cells stably expressing construct.

Figure 8: Fluorescence microscopy images showing the localization of seven different mCherry-macrodomain fusion constructs in U2OS cells stably expressing each construct. The (A) empty vector shows no distinct localization phenotype; the different macrodomains tested, including (B) the archaeal macrodomain Af1521, (C) the macrodomain from the Sindbis virus, and the macrodomains of the human proteins (D) PARP14, (E) PARP14 with G188E mutation in the previously discovered ADP-ribose binding pocket, (F) PARP15, and (G) PARP9, show diverse phenotypes. Construct expression was induced via doxycycline exposure.

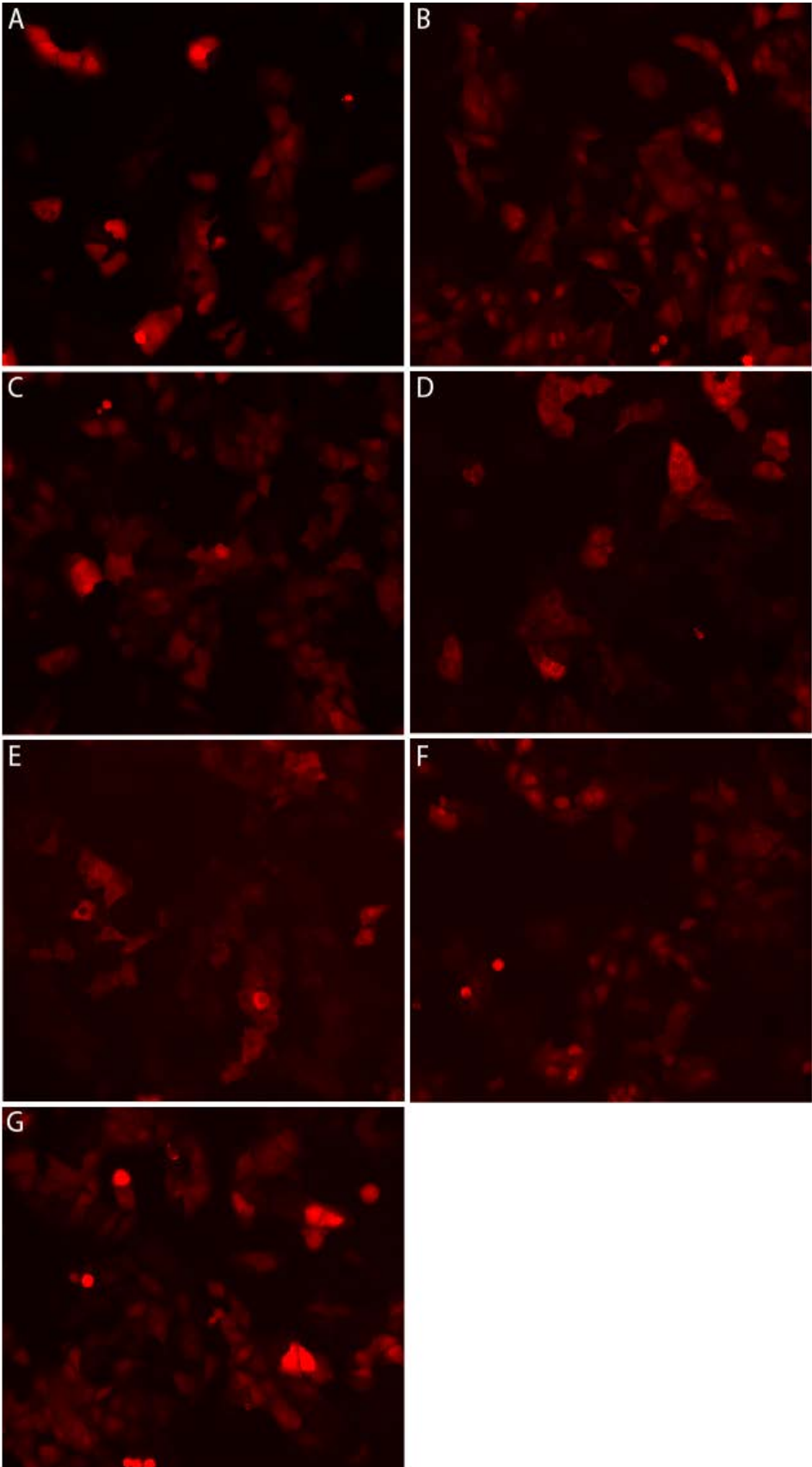


Figure 9: Fluorescence microscopy images of Huh7 cells transiently transfected with vectors encoding different mCherry-macrodomain fusion constructs showing that the nuclear-exclusion phenotype of the three PARP14 macrodomains is mediated by the second macrodomain of PARP14. Different combinations of the three macrodomains of PARP14, including (A) macro 1, (B) macro 2, (C) macro 3, (D) macros 1 and 2, and (E) macros 2 and 3 were cloned into the pDL2259 expression vector; these plasmids were then transiently transfected into Huh7 cells, and the resulting localizations were observed. Note that all constructs containing macro 2 (B, D, and E) show nuclear exclusion phenotype, whereas all others do not.

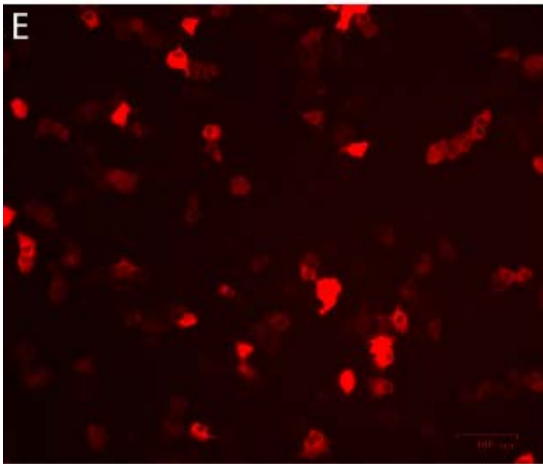
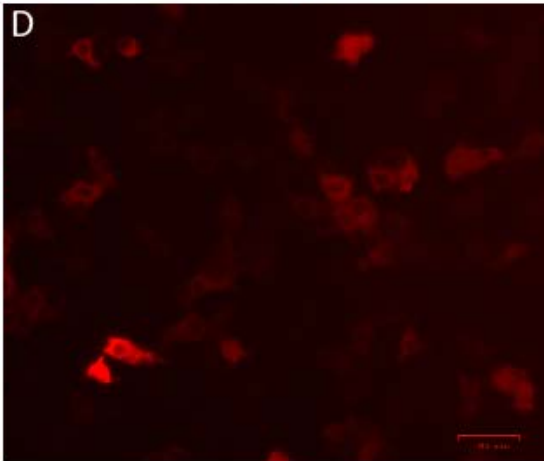
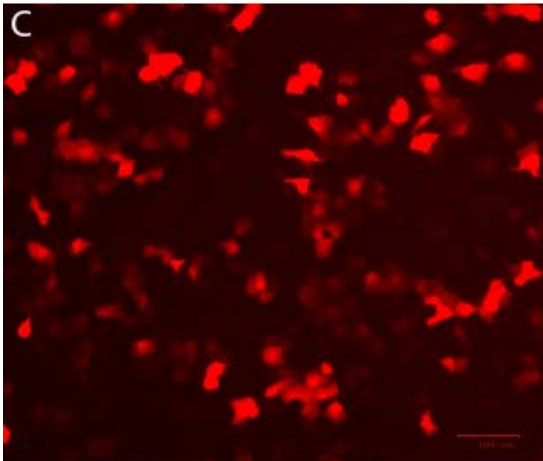
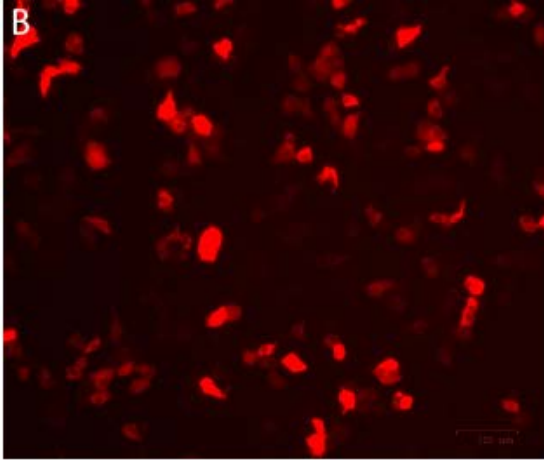
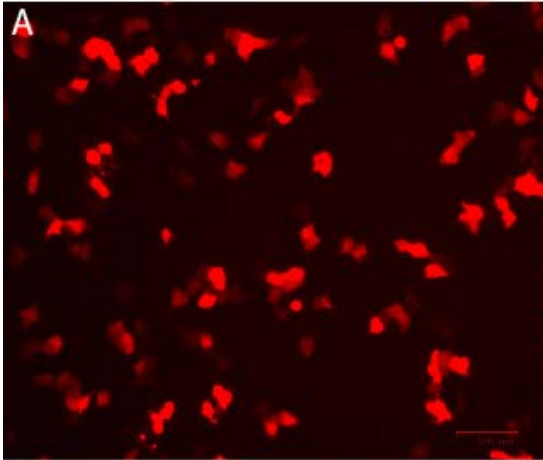
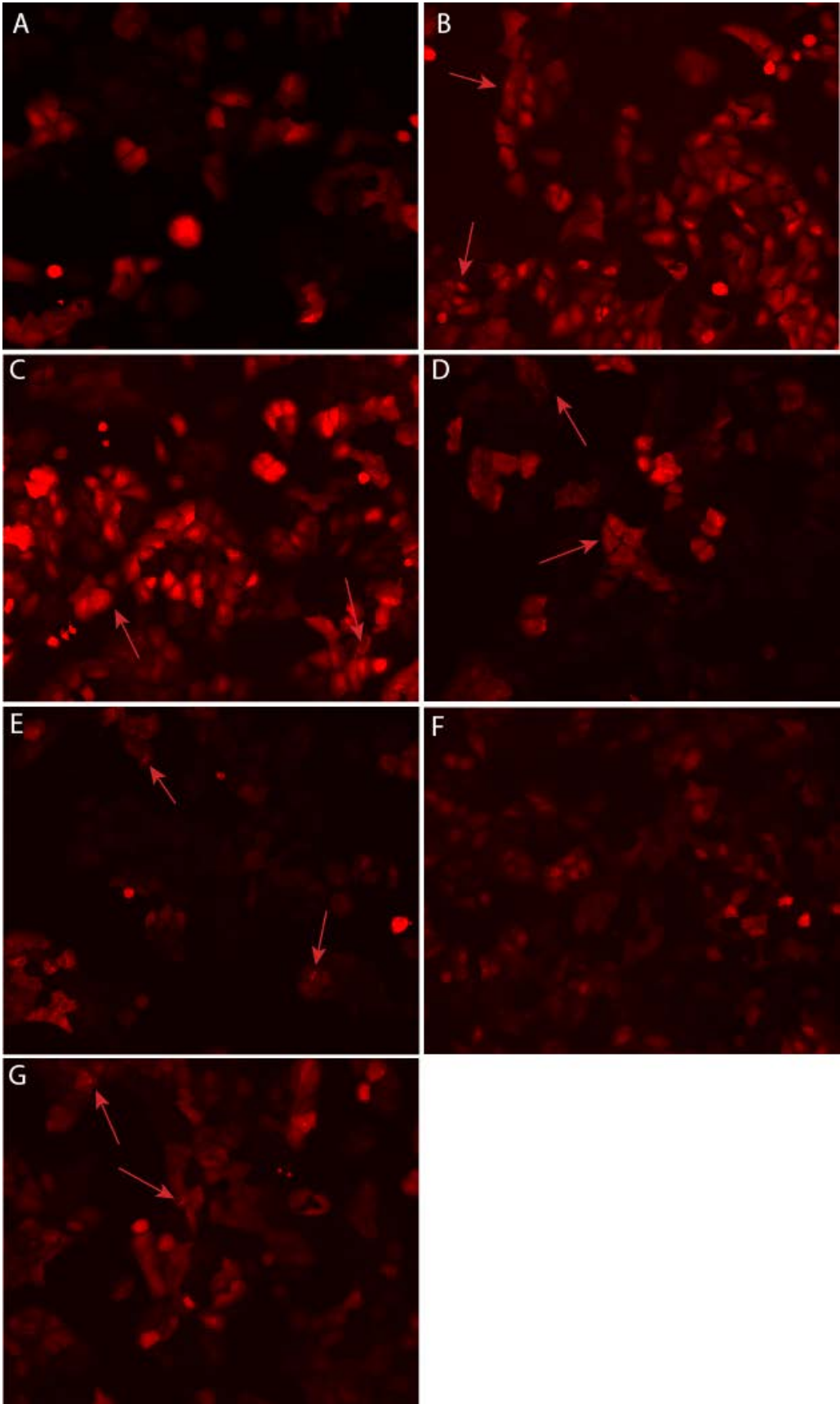


Figure 10: Fluorescence microscopy images showing the localization of seven different mCherry-macrodomain fusion constructs in U2OS cells following incubation in 0.5mM sodium arsenite for 1 hour. (A) corresponds to the empty vector, (B) to the archaeal macrodomain Af1521, (C) to the macrodomain from the Sindbis virus, (D) to the three macrodomains of PARP14, (E) to the three macrodomains of PARP14 with G188E mutation, (F) to the two macrodomains of PARP15, and (G) to the two macrodomains of PARP9. Note that all constructs except the empty vector and that containing the macrodomains of PARP15 show bright spots; examples of these are indicated by red arrows. Cells were induced to express constructs via exposure to doxycycline.



REFERENCES:

- Aguilera-Gomez, A., Oorschot, M. M., Veenendaal, T., and Rabouille, C. (2016). "In vivo visualisation of mono-ADP-ribosylation by dPARP16 upon amino-acid starvation." *ELife*, 5. doi:10.7554/elife.21475.
- Barkauskaite, E., Jankevicius, G., Ladurner, A. G., Ahel, I., and Timinszky, G. "The Recognition and Removal of Cellular Poly(ADP-Ribose) Signals." *FEBS Journal*, vol. 280, no. 15, 2013, pp. 3491–3507., doi:10.1111/febs.12358.
- Berger, W., Steiner, E., Grusch, M., Elbling, L., and Micksche, M. (2009) "Vaults and the major vault protein: novel roles in signal pathway regulation and immunity." *Cell Mol Life Sci*, 66: 43–61.
- Bick, M. J., Carroll, J. W., Gao, G., Goff, S. P., Rice, C. M., and MacDonald, M. R. (2003) "Expression of the zincfinger antiviral protein inhibits alphavirus replication." *J Virol*, 77: 11555–11562. 26.
- Bornhorst, J. A., and J. J. Falke. "Purification of proteins using polyhistidine affinity tags." *Methods in Enzymology*, vol. 326 (2000): 245-54.
- Camicia, R., Bachmann, S.B., Winkler, H.C., Beer, M., Tinguely, M., Haralambieva, E., and Hassa, P.O. "BAL1/ARTD9 Represses the Anti-Proliferative and pro-Apoptotic IFN γ -STAT1-IRF1-p53 Axis in Diffuse Large B-Cell Lymphoma." *Journal of Cell Science*, vol. 126, no. 9, 2013, pp. 1969–1980., doi:10.1242/jcs.118174.
- Chen, J., Lam, A. T., and Zhang, Y. (2018). "A macrodomain-linked immunosorbent assay (MLISA) for mono-ADP-ribosyltransferases." *Analytical Biochemistry*, 543, 132-139. doi:10.1016/j.ab.2017.12.019
- Cho, S.H., Goenka, S., Henttinen, T., Gudapati, P., Reinikainen, A., Eischen, C.M., Lahesmaa, R., and Boothby, M. "PARP-14, a Member of the B Aggressive Lymphoma Family, Transduces Survival Signals in Primary B Cells." *Blood*, vol. 113, no. 11, 2009, pp. 2416–2425., doi:10.1182/blood-2008-03-144121.
- Colicelli, J. "ABL Tyrosine Kinases: Evolution of Function, Regulation, and Specificity." *Science Signaling*, vol. 3, no. 139, 2010, doi:10.1126/scisignal.3139re6.
- Dani, N., Stilla, A., Marchegiani, A., Tamburro, A., Till, S., Ladurner, A. G., Corda, D., and Girolamo, M. D. (2009). "Combining affinity purification by ADP-ribose-binding macro domains with mass spectrometry to define the mammalian ADP-ribosyl proteome." *Proceedings of the National Academy of Sciences*, 106(11), 4243-4248. doi:10.1073/pnas.0900066106.

- Daugherty, M. D., Young, J. M., Kerns, J. A., and Malik, H. S. “Rapid Evolution of PARP Genes Suggests a Broad Role for ADP-Ribosylation in Host-Virus Conflicts.” *PLoS Genetics*, vol. 10, no. 5, 2014, doi:10.1371/journal.pgen.1004403.
- Forst, A. H., Karlberg, T., Herzog, N., Thorsell, A. G., Gross, A., Feijs, K.L., Verheugd, P., Kursula, P., Nijmeijer, B., Kremmer, E., Kleine, H., Ladurner, A.G., Schüler, H., and Lüscher, B. “Recognition of Mono-ADP-Ribosylated ARTD10 Substrates by ARTD8 Macrodomains.” *Structure*, vol. 21, no. 3, 2013, pp. 462–475., doi:10.1016/j.str.2012.12.019.
- Gao, G., Guo, X., and Goff, S.P. (2002) “Inhibition of retroviral RNA production by ZAP, a CCCH-type zinc finger protein.” *Science*, 297: 1703–1706. 24.
- Gorbalenya, A.E., Koonin, E.V., and Lai, M.M. “Putative Papain-Related Thiol Proteases of Positive-Strand RNA Viruses Identification of Rubi- and Aphthovirus Proteases and Delineation of a Novel Conserved Domain Associated with Proteases of Rubi-, α - and Coronaviruses.” *FEBS Letters*, vol. 288, no. 1-2, 1991, pp. 201–205., doi:10.1016/0014-5793(91)81034-6.
- Gruhler, A., and O. N. Jensen. “Proteomic Analysis of Post-Translational Modifications by Mass Spectrometry.” *Plant Proteomics*, 2003, pp. 33–53., doi:10.1002/9780470988879.ch2.
- Iwata, H., Goettsch, C., Sharma, A., Ricchiuto, P., Goh, W. W., Halu, A., Yamada, I., Yoshida, H., Hara, T., Wei, M., Inoue, N., Fukuda, D., Mojcher, A., Mattson, P. C., Barabási A. L., Boothby, M., Aikawa, E., Singh, S.A., and Aikawa, M. “PARP9 And PARP14 Cross-Regulate Macrophage Activation via STAT1 ADP-Ribosylation.” *Nature Communications*, vol. 7, no. 1, 2016, doi:10.1038/ncomms12849.
- Jankevicius, G., Hassler, M., Golia, B., Rybin, V., Zacharias, M., Timinszky, G., and Ladurner, A.G. “A family of macrodomain proteins reverses cellular mono-ADP-ribosylation.” *Nature Structural & Molecular Biology*, vol. 20, no. 4, 2013, pp. 508–514., doi:10.1038/nsmb.2523.
- Karras, G., Buhecha, H., Allen, M., Pugieux, C., Sait, F., Ladurner, M., and Andreas, G. (2004). “The Macro domain is an ADP-ribose binding module.” *The EMBO Journal*, 24(11), 1911-1920. doi:10.2210/pdb2bfr/pdb.
- Krishnakumar, R., and W. L. Kraus. “The PARP Side of the Nucleus: Molecular Actions, Physiological Outcomes, and Clinical Targets.” *Molecular Cell*, vol. 39, no. 1, 2010, pp. 8–24., doi:10.1016/j.molcel.2010.06.017.
- Lange, A., Mills, R.E., Lange, C.J., Stewart, M., Devine, S.E., and Corbett, A.H. “Classical nuclear localization signals: definition, function, and interaction with importin alpha.”

The Journal of Biological Chemistry, vol. 282,8 (2006): 5101-5.
doi:10.1074/jbc.R600026200.

- Lee, M.K., Cheong, H.S., Koh, Y, Ahn, K. S., Yoon, S. S., and Shin, H. D. “Genetic Association of PARP15 Polymorphisms with Clinical Outcome of Acute Myeloid Leukemia in a Korean Population.” *Genetic Testing and Molecular Biomarkers*, vol. 20, no. 11, 2016, pp. 696–701., doi:10.1089/gtmb.2016.0007.
- Legube, G. and D. Trouche. “Regulating Histone Acetyltransferases and Deacetylases.” *EMBO Reports*, vol. 4, no. 10, 2003, pp. 944–947., doi:10.1038/sj.embor.embor941.
- Leung, A. K., Vyas, S., Rood, J. E., Bhutkar, A., Sharp, P.A., and Chang, P. “Poly(ADP-ribose) regulates stress responses and microRNA activity in the cytoplasm.” *Molecular cell* vol. 42,4 (2011): 489-99. doi:10.1016/j.molcel.2011.04.015.
- Li, C., Debing, Y., Jankevicius, G., Neyts, J., Ahel, I., Coutard, B., and Canard, B. “Viral Macro Domains Reverse Protein ADP-Ribosylation.” *Journal of Virology*, vol. 90, no. 19, 2016, pp. 8478–8486., doi:10.1128/jvi.00705-16.
- Li, N., and J. Chen. “ADP-Ribosylation: Activation, Recognition, and Removal.” *Molecules and Cells*, vol. 37, no. 1, 2014, pp. 9–16., doi:10.14348/molcells.2014.2245.
- Mao, R., Nie, H., Cai, D., Zhang, J., Liu, H., Yan, R., Cuconati, A., Block, T. M., Guo, J. T., and Guo, H. (2013) “Inhibition of hepatitis B virus replication by the host zinc finger antiviral protein.” *PLoS Pathog*, 9: e1003494.
- Mehrotra, P., Riley, J. P., Patel, R., Li, F., Voss, L., and Goenka, S. “PARP-14 Functions as a Transcriptional Switch for Stat6-Dependent Gene Activation.” *Journal of Biological Chemistry*, vol. 286, no. 3, 2010, pp. 1767–1776., doi:10.1074/jbc.m110.157768.
- Morazzani, E. M., Compton, J. R., Leary, D. H., Berry, A. V., Hu, X., Marugan, J. J., Glass, P. J., and Legler, P. M. “Proteolytic Cleavage of Host Proteins by the Group IV Viral Proteases of Venezuelan Equine Encephalitis Virus and Zika Virus.” *Antiviral Research*, vol. 164, 2019, pp. 106–122., doi:10.1016/j.antiviral.2019.02.001.
- Muller, S., Moller, P., Bick, M. J., Wurr, S., Becker, S., Gunther S., and Kummerer, B. M. (2007) “Inhibition of filovirus replication by the zinc finger antiviral protein.” *J Virol*, 81: 2391–2400. 25.
- Park, E., and D. E. Griffin. “The nsP3 macro domain is important for Sindbis virus replication in neurons and neurovirulence in mice.” *Virology*, vol. 388,2 (2009): 305-14. doi:10.1016/j.virol.2009.03.031.
- Pawson, T., and G. D. Gish. “SH2 And SH3 Domains: From Structure to Function.” *Cell*, vol. 71, no. 3, 1992, pp. 359–362., doi:10.1016/0092-8674(92)90504-6.

- Perina, D., Mikoč, A., Ahel, J., Četković, H., Žaja, R., and Ahel, I. “Distribution of protein poly(ADP-ribosyl)ation systems across all domains of life” *DNrepair*, vol. 23 (2014): 4-16.
- Rack, J. G., Perina, D., and Ahel, I. “Macrodomains: Structure, Function, Evolution, and Catalytic Activities.” *Annual Review of Biochemistry*, vol. 85, no. 1, 2016, pp. 431–454., doi:10.1146/annurev-biochem-060815-014935.
- Ran, X., Ao, Z., and Yao, X. “Apobec3G-Based Strategies to Defeat HIV Infection.” *Current HIV Research*, vol. 14, no. 3, 2016, pp. 217–224., doi:10.2174/1570162x14999160224100541.
- Schlick, K. H., Lange, C. K., Gillispie, G. D., and Cloninger, M. J. “Characterization of protein aggregation via intrinsic fluorescence lifetime.” *Journal of the American Chemical Society* vol. 131,46 (2009): 16608-9. doi:10.1021/ja904073p.
- Teloni, F., and M. Altmeyer. “Readers of Poly(ADP-Ribose): Designed to Be Fit for Purpose.” *Nucleic Acids Research*, vol. 44, no. 3, 2015, pp. 993–1006., doi:10.1093/nar/gkv1383.
- Timinszky, G., Till, S., Hassa, P. O., Hothorn, M., Kustatscher, G., Nijmeijer, B., Colombelli, J., Altmeyer, M., Stelzer, E. H., Scheffzek, K., Hottiger, M. O., and Ladurner, A. G. “A Macrodomain-Containing Histone Rearranges Chromatin upon Sensing PARP1 Activation.” *Nature Structural & Molecular Biology*, vol. 16, no. 9, 2009, pp. 923–929., doi:10.1038/nsmb.1664.
- Vivelo, C. A., and A. K. Leung. “Proteomics approaches to identify mono-(ADP-ribosyl)ated and poly(ADP-ribosyl)ated proteins.” *Proteomics* vol. 15,2-3 (2014): 203-17. doi:10.1002/pmic.201400217.
- Wang, R., and M. G. Brattain. “The Maximal Size of Protein to Diffuse through the Nuclear Pore Is Larger than 60 KDa.” *FEBS Letters*, vol. 581, no. 17, 2007, pp. 3164–3170., doi:10.1016/j.febslet.2007.05.082.
- Xu, Y., Zhang, S., Lin, S., Guo, Y., Deng, W., Zhang, Y., and Xue, Y. “WERAM: a Database of Writers, Erasers and Readers of Histone Acetylation and Methylation in Eukaryotes.” *Nucleic Acids Research*, vol. 45, no. D1, Jan. 2017, pp. 264–270., doi:10.1093/nar/gkw1011.
- Yu, M., Schreek, S., Cerni, C., Schamberger, C., Lesniewicz, K., Poreba, E., Vervoorts, J., Walsemann, G., Grötzinger, J., Kremmer, E., Mehraein, Y., Mertsching, J., Kraft, R., Austen, M., Lüscher-Firzlaff, J., and Lüscher, B. “PARP-10, a Novel Myc-Interacting Protein with Poly(ADP-Ribose) Polymerase Activity, Inhibits Transformation.” *Oncogene*, vol. 17, no. 24, ser. 12, 17 Mar. 2005. 12.

- Zhang, Y., Mao, D., Roswit, W. T., Jin, X., Patel, A. C., Patel, D. A., Agapov, E., Wang, Z., Tidwell, R. M., Atkinson, J. J., Huang, G., McCarthy, R., Yu, J., Yun, N. E., Paessler, S., Lawson, T. G., Omattage, N. S., Brett, T. J., and Holtzman, M. J. “PARP9-DTX3L Ubiquitin Ligase Targets Host Histone H2BJ and Viral 3C Protease to Enhance Interferon Signaling and Control Viral Infection.” *Nature Immunology*, vol. 16, no. 12, 2015, pp. 1215–1227., doi:10.1038/ni.3279.
- Zhou, S. “SH2 Domains Recognize Specific Phosphopeptide Sequences.” *Cell*, vol. 72, no. 5, 1993, pp. 767–778., doi:10.1016/0092-8674(93)90404-e.